BEST: International Journal of Management Information Technology and Engineering (BEST: IJMITE)
ISSN (P): 2348–0513, ISSN (E): 2454–471X
Vol. 9, Issue 2, Dec 2021, 131–148
© BEST Journals

UAV IMPACT SIMULATION AND ANALYSIS ON THE BASE OF EQUIVALENT AIRCRAFT PERFORMANCE

AYUBU JACKSON SAITABAU, TAFADZWA GERALD KAPESA & SU-YAN, T. DMYTRO

Department of Civil Aviation, Nanjing University of Aeronautics and Astronautics, Nanjing, China

ABSTRACT

The future of technology is dependent on UAVs; the forecast is that they will bring about a new era in the market and revolutionize the technology in most aspects of life. Most UAVs are being used by commercial entities such as agriculture, logistics and infrastructures [18]. The trend in technology is mainly on increasing endurance, payload, advancement in the symbiotic interaction between man and drones and putting a solid ground and principles for the safe handling of UAVs. However, that being the case, the airborne collision safety between nose section aluminum component part of a transport aircraft and the UAV under different aircraft flight conditions, taking into consideration a detailed background analysis of the aircraft performance is taken into account in this paper and help get a clear depiction of the results simulated under ABAQUS/EXPLICIT2020 software.

KEYWORDS: UAV (drone),Impact, Aluminum, Airworthiness, Simulation, FEM analysis.

NOMENCLATURE

E Young’s modulus.

V Poisson’s ratio.

A,B, n, m Material constants for JC material model.

Tm Melting temperature.

To Reference temperature.

ε̇o Reference strain rate.

ρ Density.

Cp Specific heat.

D1, D2, D3, D4, D5 Johnson’s cook failure model parameters.

Abbreviations

MSL Mean Sea Level.

UAV Unmanned Aerial Vehicle.

FAR Federal Aviation Regulation.

KE Kinetic Energy.

ALLPD Plastic deformation for whole model.

ALLKE Kinetic Energy for Whole Model.

ALLVD Viscous Dissipation for whole model.

ALLDMD Damage Dissipation Energy for whole model.

EI Internal Energy.

EV Viscous Energy Dissipated.

EFD Frictional Dissipated Energy.

EKE Kinetic Energy.

EIHE Internal Heat Energy.

EW Work done by External applied loads.

EPW Work done by Contact Penalties.

ECW Work done by Constraint penalties.

EMW Work done by Propelling added mass.

EHF External Energy through external fluxes.

EE Recoverable Elastic Strain Energy.

EP Dissipated Energy through inelastic processes.

ECD Dissipated Energy through Viscosity or Creep.

EA Artificial Strain Energy.

EDMD Dissipated Energy through Damage.

EDC Dissipated Energy through Distortion.

EFC Fluid Cavity Energy.

1. INTRODUCTION

The advancements in UAVs have brought about a serious drive in the civil and military aviation industry for years now, mainly in the north America. Goraj [1]pointed that currently the drone market is highly conducted by mostly the military at an estimated growth in the economy target of $82.1 billion by end of 2025 [2]. The main applications of UAVs in the military include reconnaissance, transport, and search and rescue, other applications apart from the military include agricultural use, power line inspection, aerial photography and video production. A report provided by the United States Department of Defense (DoD) underlined some few significant advancements required for different UAVs [3]. These advancements may be backed up by the current state-of-the-art technology. As the United States DoD builds more multi-functional drones and other states are following the same strategies and are participating in purchasing such systems.

UAV collisions present a possible risk source to the safety of civil air transport, however for tolerance to be ensured the UAV and aircraft structures have to fulfil the airworthiness requirements put by FAA. According to FAR 25, Sub-part 25.571, flap structures of large transport aircraft have to overcome an impact with a 4 lb. [18.a] UAV at usual operating speeds [4].

Even though the airworthiness authorities in different states have some regulations monitoring the activities of drones, the incidents that have been reported and recorded have indicated some faults of such regulations; in addition, the airworthiness requirements of aircraft when it comes to high-speed UAV impact hasn't been taken into consideration during design and manufacturing. Making the possibility of high-speed collision between aircraft and UAVs existent, whereas the safety risks are left not known. Therefore, evaluations of air borne impacts between drones and commercial aircrafts with advancements in technology and simulations are suggested necessary to reduce future catastrophic incidents.[18]

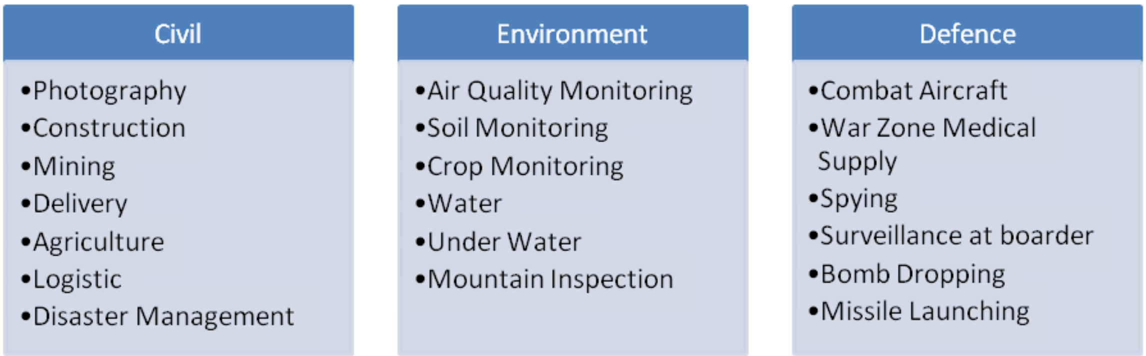

Figure 1: Potential Drone Applications.

Various works can be found in literature covering a wide range with drone collision indicating the catastrophic impacts on the most important structural areas which can experience this casualties: The windshield (Plassard et al., 2015; Lu et al., 2015; Ugrcic et al., 2015) and the wing leading edge (Sun et al., 2010; Guida et al., 2008; Smojver and Ivancevic, 2010; Wang and Yue, 2010; Hanssen et al., 2006; Airoldi and Cacchione, 2006; Johnson and Cook, 1983; 1985; Johnson and Cook, 1985; Liu et al., 2013a; Liu and Sun, 2014; Lavoie et al., 2007a; Liu et al., 2013b; Jain and Ramachandra, 2003; Guida et al., 2011).

2. RESEARCH OBJECTIVES

Simulation and analysis of the UAV collision on a plate (airframe structure). The use of Abaqus software to model and simulate at different crash scenarios and conditions. Contribution positively to the gap left by previous researchers on the informative data and results achieved from the simulation and model analysis. Showing the performance of the UAV drone at different mass, speed, acceleration during the strike of airplane / plate at various angles (landing and taking off scenarios). Based on the results of the above-mentioned study, the UAV at varied capabilities) drone impact damage mitigation measures will proposed.

2.1 Background Analysis of Aircraft Flight Performances on basis of FAR 91

Three predicted collision velocities were rendered at the initial phase of the design, based on the following limitations. Initially, FAR 91.117 states unless authorized by the Administrator, no individual may operate an aircraft less than 10,000 feet (approximately 3,000 m) MSL at a required airspeed not exceeding 250 knots [5]. Secondly, the maximum aircraft altitude of any UAV is hindered to being 500 m from the ground by DJI. Thirdly, on basis of the FAR description Part 107

[6], small UAVs are prohibited to being operating over 400 feet (approximately 120 m). Moreover, the flight parameters of an aircraft considered in this research were taken into account. Therefore, the three expected relative velocities of impact were 200 m/s, 171 m/s, and 116 m/s respectively from largest to smallest at various flight levels, including the average velocities of the UAV being approximately 20 m/s. [18]

Some specific parameters for the drone and aircraft are present in Table 1.

Table 1: Relative Velocity and Altitude

Altitude/Wind Speed	Aircraft Speed	UAV speed	Relative speed
121m	96m/s	20m/s	116m/s
500m	151m/s	20m/s	171m/s
125knots	180m/s	20m/s	200m/s

1.2 Aircraft Flight Performance at Various Phases and Speed

During the takeoff, climbing and landing the aircraft can face some not so much catastrophic after effects of UAV/bird collision and lead to a number of different structural damage. The main aim of this paper being to go into detail and find out at what phase (based on pitch angle) and speed of the airplane the collision can be most detrimental to the integrity of the aircraft structure.

The case study based more on the Boeing 787 which is considered as the most sophisticated aircraft which has incorporated some of the state-of-the-art technology from various fields including military with a cruising altitude of up to 45,000ft at almost 800km/h.

This research is very important due to so many reasons and the most important being the advancement of airplane structure which is focused more on the passenger safety, be there come any impact on the structure of the airplane such as bird or drone impact at lower operational altitudes.

As it is known the airplane has 4 phases namely takeoff, climb, cruising and descending (landing), the most detrimental phase being climb and descending which in turn means the airplane is operating at low altitude mainly in an atmospheric layer that other aerial vehicles are operating at and at climbing phases the impact being much more than during descending where the airplane operates at full speed (full throttle power). When the UAV impacts the airplane at an angle of 15˚ which is considered to being the maximum pitch angle during takeoff and there is energy lost which can be in the form of plastic dissipation energy (ALLPD for the whole model), damage dissipation energy (ALLDMD for the whole model), viscous dissipation energy (ALLVD of the whole model), kinetic energy lost (ALLKE for the whole model)[19], all these energy will be considered for the analytical results to better understand the damage level and better ways to mitigate the effects by the manufacturers. During landing the airplane is prone to pitching angles of up to 33˚ and this is also considered during the simulations in ABAQUS software.

3. MATERIAL SELECTIONS

3.1 Aircraft(A2024-T351).

The material applied to the aircraft(plate) was based on the history of aluminum. Aluminum alloys have always been in the front seats as a material for commercial and military aircraft for almost 80 years due to their characteristic's mechanical properties, easily formable with design, mature manufacturing processes and inspection criteria, and remains so for a long time before another material comes in place with better properties to be constituted in place of weight loss with efficiency on the airplane. Never the less, non-metallic materials, despite the problems mentioned earlier, because of their dominating specific strength properties provide a very competitive alternative, hence producers of aluminum need to keep a close watch out by investing and contributing on a greater deal of effort on enhancing the thermo-mechanical properties of aluminum alloys produced.

During the metamorphic design stage of Boeing 777, aluminum producers were posed with a question for the few adjustments example for the upper-wing surface and fuselage. A higher compressive yield strength was required for the upper wing surface. High corrosion resistance also was a primary requirement. When it comes to the fuselage, enhanced damage tolerance and durability than the incumbent 2024-T3 was needed. Aluminum producers accounting for the designer's requirement came up with the 7055-T7751 plate and 7055-T77511 extrusions for the upper wing surface, and Alclad 2524-T3 (Table 2) sheet and 2524-T351 plate to be used on the fuselage skin. They also developed 7150-T7751 extrusions for the supporting members of the fuselage structure. Boeing 777 saved a lot of money on weight after the application of these materials [7,20] (Figure 2).

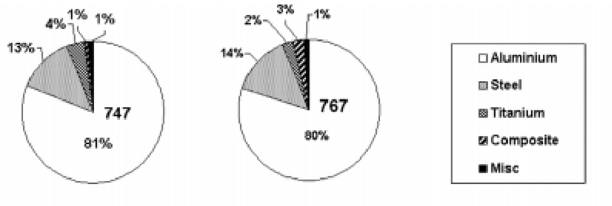

a)

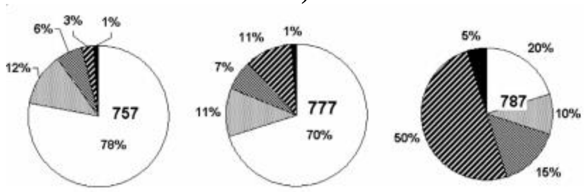

b)

Figure 2: Material Combination used in Boeing Aircrafts. The figure is based on [20].

Table 2: Mechanical Properties and Johnson's Cook Failure Model Parameters for A2024-T351

Parameter Elasticity	AA2024-T351
E(Gpa)	70
v(-)	0.3
Thermoviscoplastic behavior	
A(MPa)	352
B(MPa)	440
n(-)	0.42
$\dot{\varepsilon}_o$	3.3e-4
Other physical Constants	
ρ (Kg/m^3)	2700
ß(-)	0.9
Cp(J/Kgk)	900
To(K)	293
Tm(K)	275
Parameter	AA2024-T351
D1	0.13
D2	0.13

D3	-1.5
D4	0.011
D5	0

3.2 UAV (A7075-T651)

As days goes by the demand for energy-absorbing lightweight engineering structures for blast and impact applications in automotive, aeronautical and defense industry is growing at an increasingly fast pace [11].

The UAV material was assigned using a user-defined cohesive element taking into account both the strength and toughness when the debonding occurs under transverse interface compression, together with no-frictional effects after full debonding with A7075-T651.

On the basis of numerical simulations, various aspects have to be taken under the microscope, such are as initiation of damage (Johnson and Cook, 1983; 1985; Xue and Wierzbicki, 2009; Liu 2013a; Liu and Sun, 2014), contact behavior (Johnson and Cook, 1983; 1985) and drone modelling and simulation approaches (Lavoie 2007a; Liu 2013b; Jain and Ramachandra, 2003; Guida 2011; Liu 2008).

Moreover, to design structures that can withstand UAV impact, knowledge on impact scenario has to be enhanced by experimental initiations and numerical simulations. Due to impact initiation tests, the drone impact events, can be expensive and time consuming, it becomes necessary to advance the numerical Finite Element Models that are able to understand and visualize as well as assimilate the high velocity collision phenomena of the aircraft structure.

Table 3: Mechanical Properties and Johnson's Cook Failure Model Variables for A7075-T651 [8-10]

Material Properties	AA7075-T651
Density ρ (Kg/m^3)	2700
Young's Modulus E(GPa)	70
Poisson's Ratio	0.3
Inelastic Heat Fraction	0.9
Specific Heat Cp(J/KgK)	910
Strain Hardening	
A(MPa)	520
B(MPa) n Strain Rate Hardening	477 0.52
Reference Strain Rate $\dot{\varepsilon}_o$ (S^{-1})	5e-4
C	0.001
Temperature Softening	
Reference Temperature Tr(K)	293
Melting Temperature Tm(K)	893
m	1
Damage Parameters	
D1	0.096
D2	0.049
D3	-3.465
D4	0.016
D5	1.099

The simulation of drone impact on aluminum is usually done by progressive dynamic failure analysis that adopts a Johnson-Cook (J-C) constitutive model material (Johnson and Cook, 1983; 1985). Many approaches have been taken into consideration on the importance of both stress and strain rates on propagation of failure have been shown in this paper.

4. COMPUTATION MODEL SETUP

4.1 UAV Modeling

The modeling of the UAV was done in Catia V5R20 (Figure 3) software and later Abaqus 2020 (Figure 4) software imported the file from Catia CATPART for further material modification and simulation. The dimensions are in millimeters and were obtained from GRABCAD engineer modeling data base, the figures below illustrate more [16].

The FE model for the UAV comprised of various parts (see Fig. below) the solid type of shell elements was used to model the motors, camera, Lithium Polymer (Li-Po) battery cells and circuit boards and shell elements to model the body, battery case, and propellers, with integrated module. The shell and solid elements are approximately 0.85 mm thick [18].

However, the UAV had some geometrical mismatch parameters and ABAQUS software prompted the user to refine the geometry by editing the validity in the part module and the software interface had options to automatically ignore the invalidity caused by the geometry. The first option was mandatory and converting the analytical data to update the validity of the geometry was achieved resulting to a successful model importation [15].

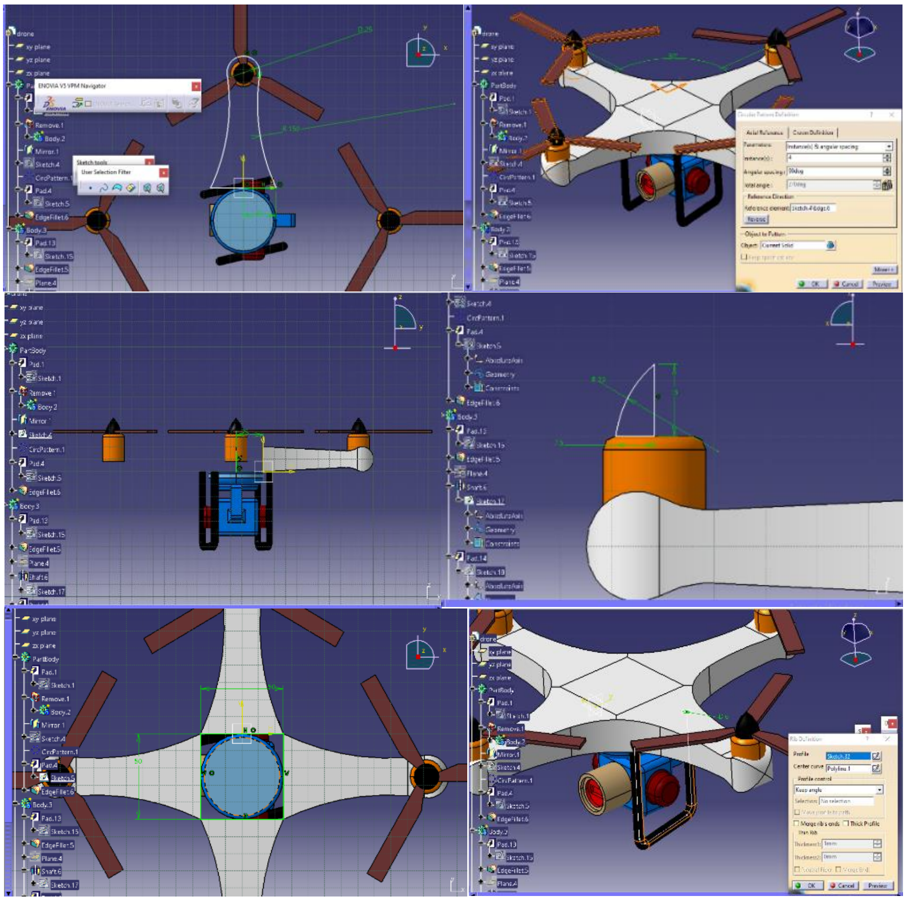

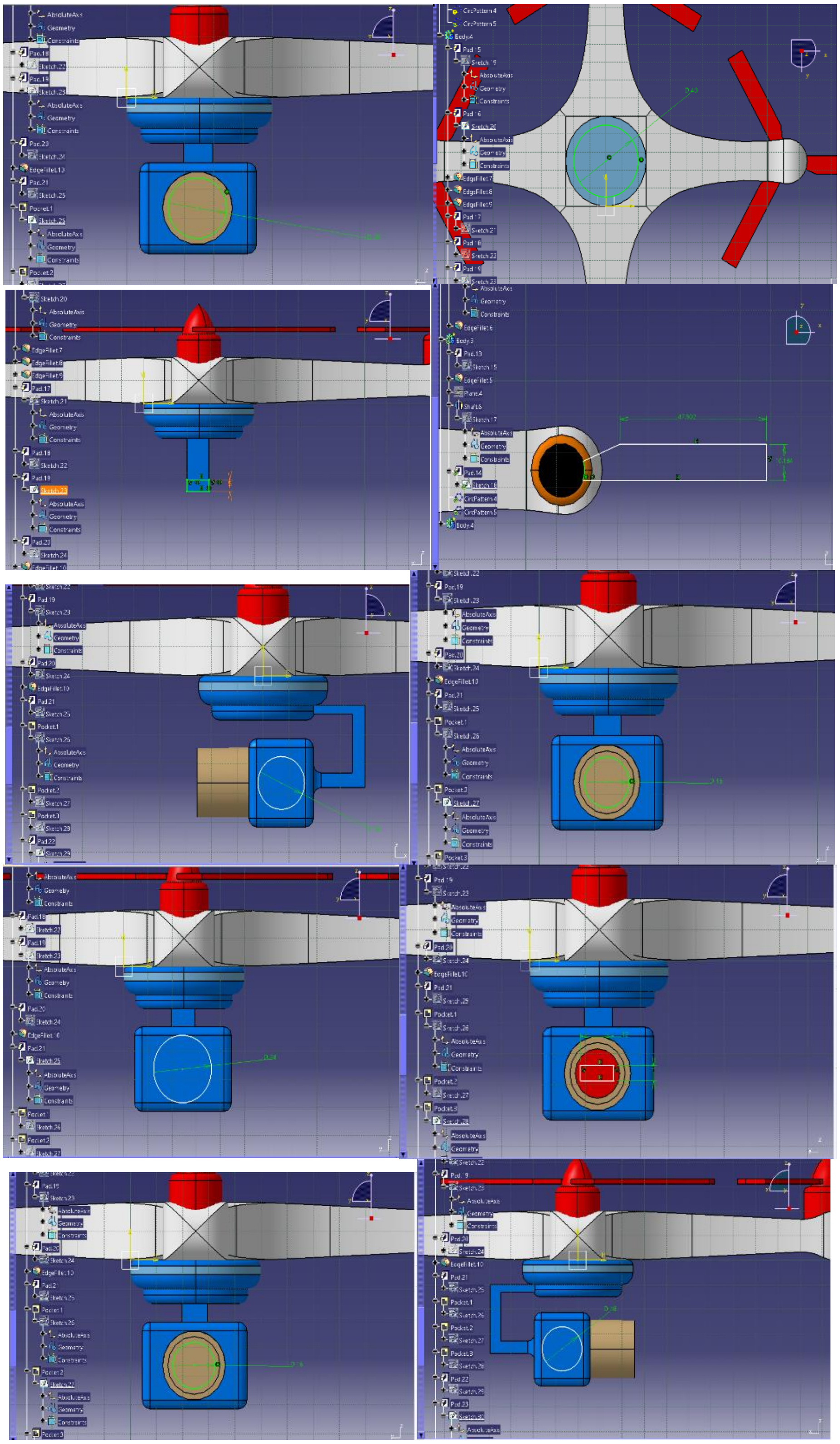

Figure 3

After modeling the design was then imported by ABAQUS from Catia data base as seen in the figure below, meshing was done after the design was imported successfully.

However, the normal meshing tradition to this design posed some challenges but yet interesting topic to study more on the meshing of a part design. The meshing strategy proposed by the Abaqus interphase was to partition, assign a Tet shape or manually meshing using the create bottom-up mesh tool which were the methods used to manually mesh the UAV model.

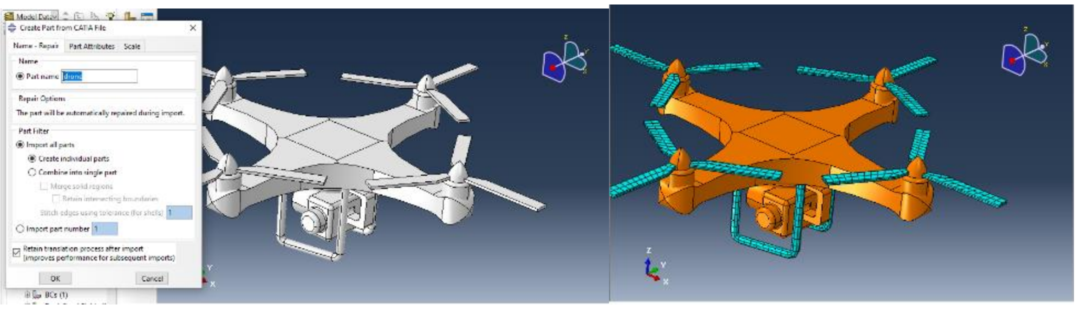

Figure 4

4.2 Aluminum Plate Modeling

For the plate design, some design variables are interrelated. The evaluation of the performance on basis of the aircraft and precomputation of all other variables are needed to change a particular design variable. The aircraft's zero-lift drag coefficient and induced drag factor are taken as variables for the design steps.

The part of the airplane that the simulation and analysis was mainly focused on is the front nose section that comprises of the windshield and radome that comes first into contact with the air particles and thus can sometimes fatally collide with objects and birds that are air borne (Figure 5).

The skin thickness of most Boeing aircrafts was specified by the manufacturer to be 0.039 in (0.99mm) thick, investigators measured the thickness at 0.035 in (0.89mm) to 0.037 in (0.94mm) this was reported according to the milling process. The set skin thickness in this article was set as 1mm which was assigned in the shell thickness of the aluminum A2024.

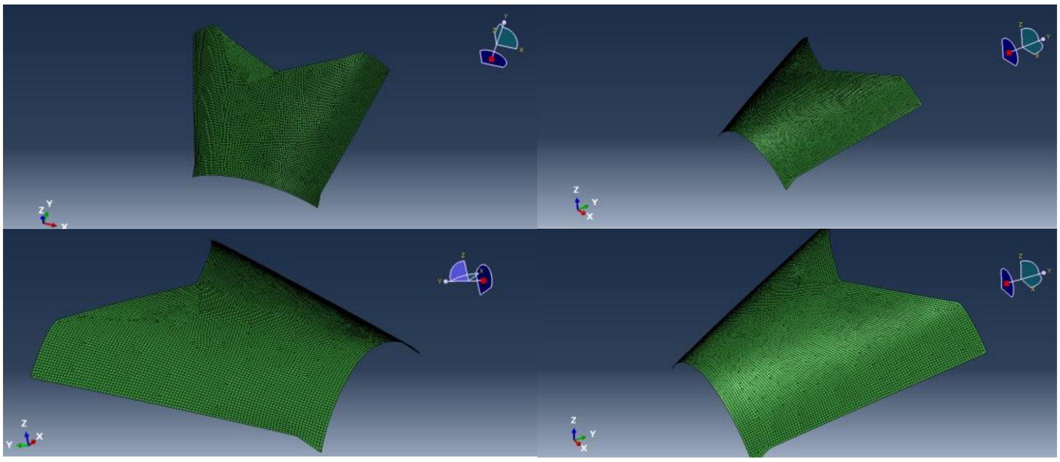

Figure 5

5 COMPUTATIONAL MODEL SIMULATE ON AND ANALYSIS USING ABAQUS 2020

The analysis was based on different conditions of the impact and the conditions (Figure 6) as explained above was at aircraft takeoff and landing where there is maximum and minimum speeds and pitch angle during flight.

The operational speeds of the drone were obtained from the exact speed that the manufacturer set the drone to operate at maximum speeds which were 116m/s, 171m/s and 200m/s and the pitch angle that the airplane(plate) was set to be at 15˚ ad 33˚.

As the UAV impact localized damage is induced around the area in which the collision takes place, analyses have been conducted on an aluminum plate that depicts the nose section of the airplane, and thus decreasing the computational time and output of the job file. For a reduction in the finite element model, an automated process has been employed that improves the original ABAQUS [15] input job file and in return provides a new input job file that has elements in the nearby impact zone. Collision impact have been conducted on several locations on the nose structure with different initial velocity vectors to simulate possible impact scenarios during takeoffs and landings [18.a].

The validity of numerical UAV strike simulations highly is dependent on the correct alignment and modelling of forces and pressures introduced to the impacted structure as seen in the graphs below different energies are an exponential decay or increase in time depending on the energy factor [18.a].

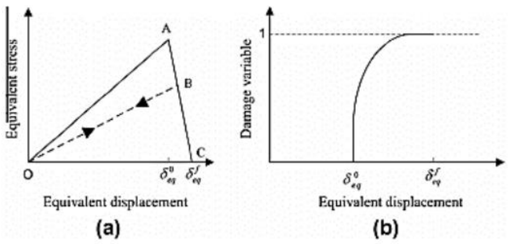

Figure 6: a) Equivalent Stress Displacement Diagram,
b) Damage Variable as a Function of Equivalent Displacement.[21].

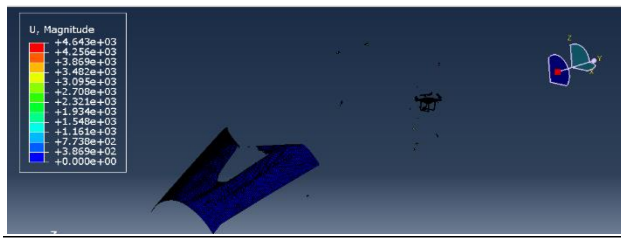

At 116m/s (Kinetic Energy lost=1.21e+09 J), (Total Energy dissipated=1.27e+9 J) & (Pitch Angle = 33˚).

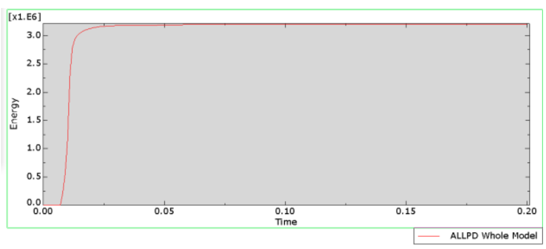

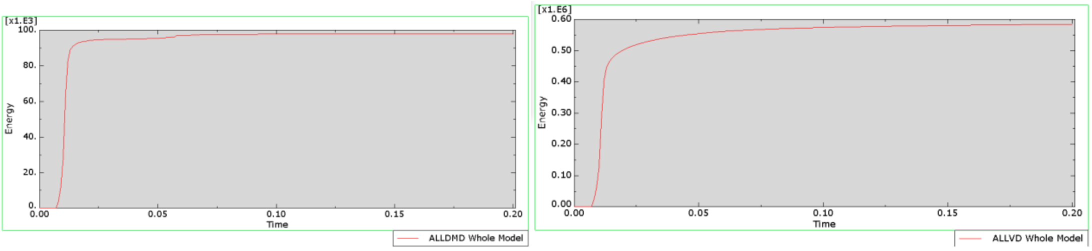

At 171m/s (Kinetic Energy lost=2.75e+09 J), (Total Energy dissipated=2.76e+09 J)& (Pitch Angle=33˚).

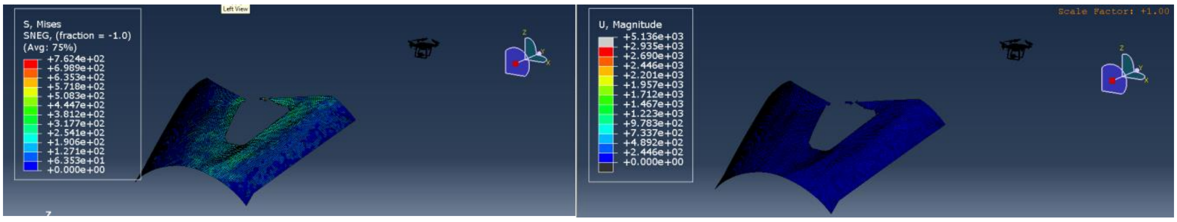

Pressure points (red points) isolated on the boundary conditions encastred when U1, U2 and U3 are all zero at a velocity of 171m/s (depicts the front side view portion of the aluminum plate).

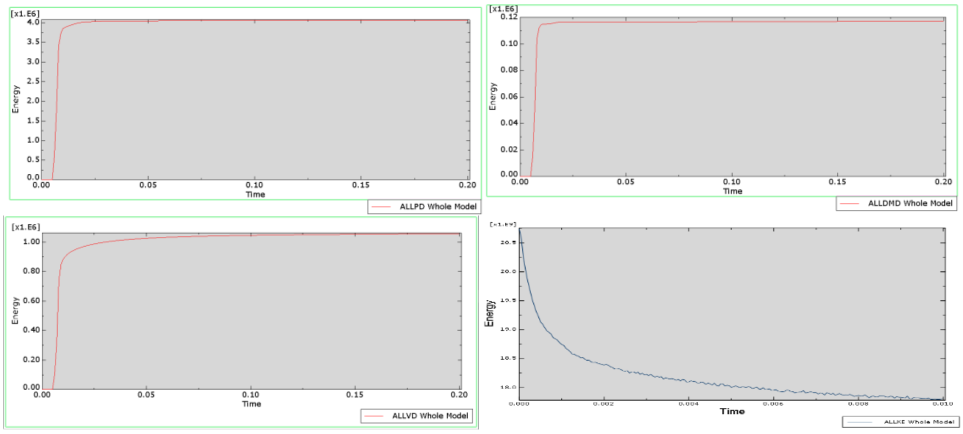

At 200m/s (Kinetic Energy lost=3.77e+09 J), (Total Energy dissipated=3.78e+09 J) & (Pitch Angle=33˚).

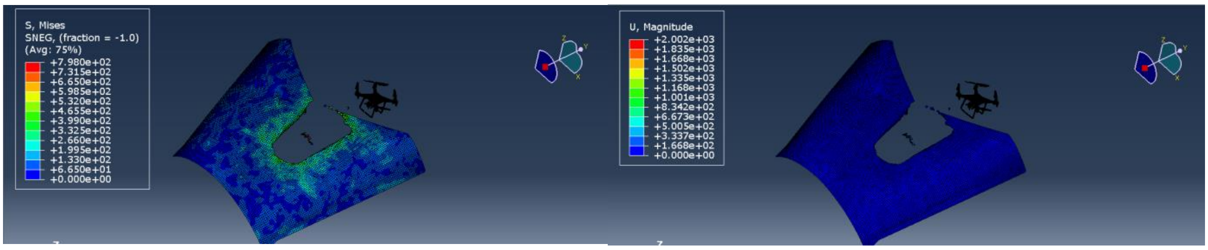

Pressure points (red points) isolated on the boundary conditions encastred when U1, U2 and U3 are all zero at a velocity of 200m/s (depicts the front side view portion of the aluminum plate).[17]

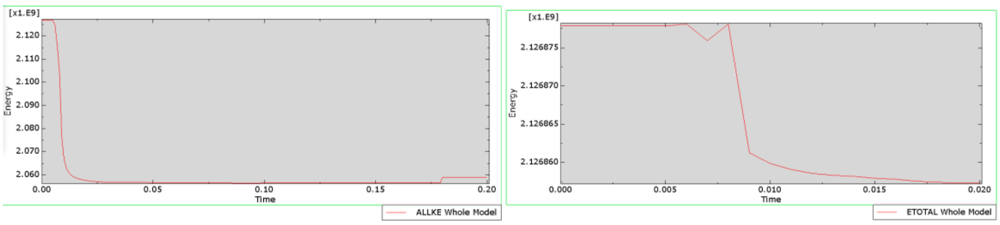

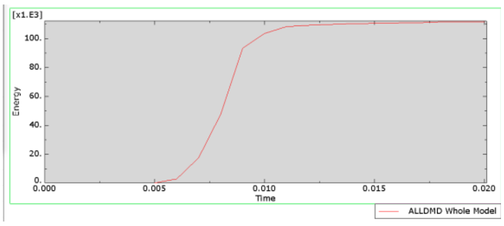

Problem size for the pitch angle of 33˚.

Number of elements is 27365

Number of nodes is 56185

Number of nodes defined by the user 31095

number of internal nodes generated by the program 25090

total number of variables in the model 226016

(Degrees of freedom plus max no. Of any Lagrange multiplier variables. Include *print, solve=yes to get the actual number.)

<u>At 116m/s</u> (Kinetic Energy lost=1.20e+09 J), (Total Energy dissipated=1.27e+9 J) & (Pitch Angle = 15˚).

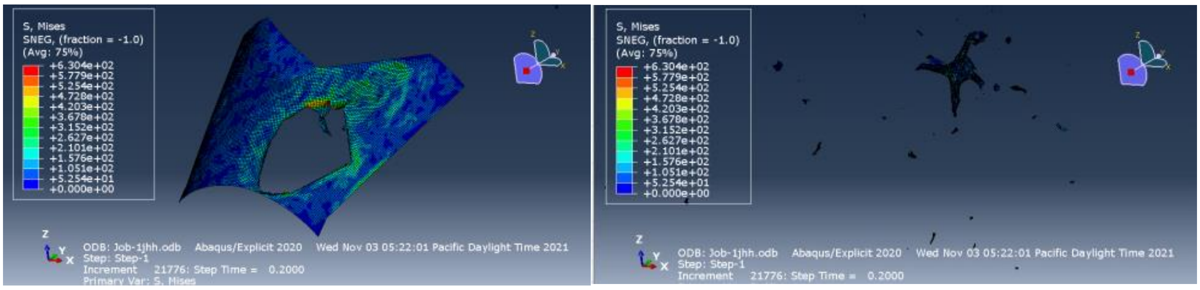

Pressure points (red points) isolated on the boundary conditions encastred when U1, U2 and U3 are all zero at a velocity of 116m/s (depicts the front side view portion of the aluminum plate and UAV segments after impact).

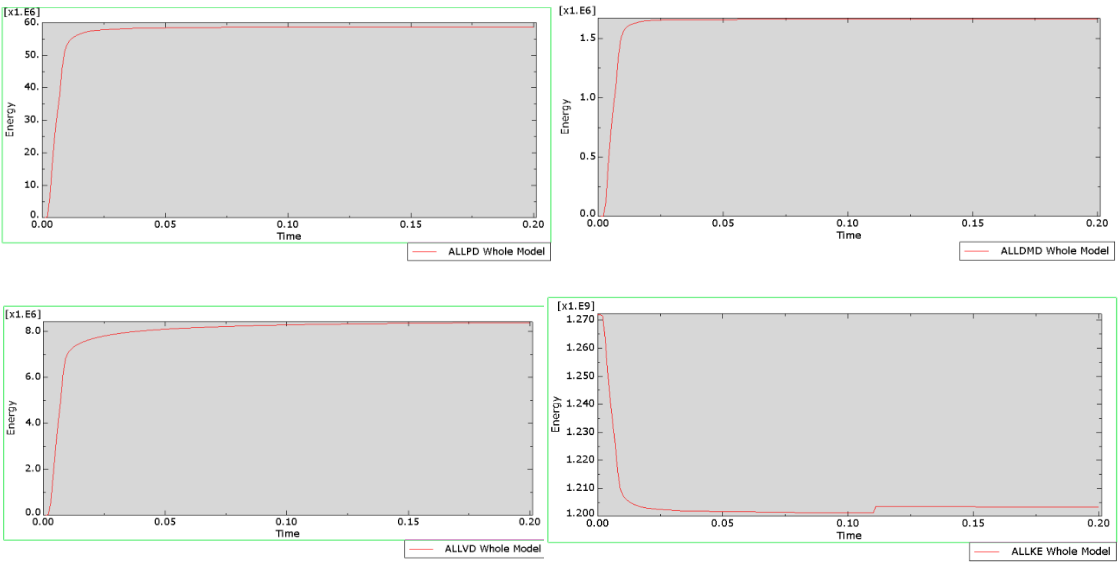

At 171m/s (Kinetic Energy lost=2.71e+09 J), (Total Energy dissipated=2.76e+9 J) & (Pitch Angle = 15˚).

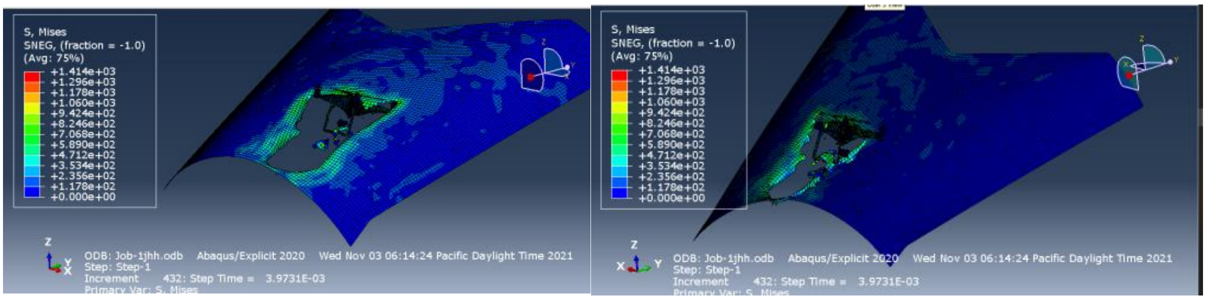

Pressure points (red points) isolated on the boundary conditions encastred when U1, U2 and U3 are all zero at a velocity of 171m/s (depicts the front and inside view portion of the aluminum plate).

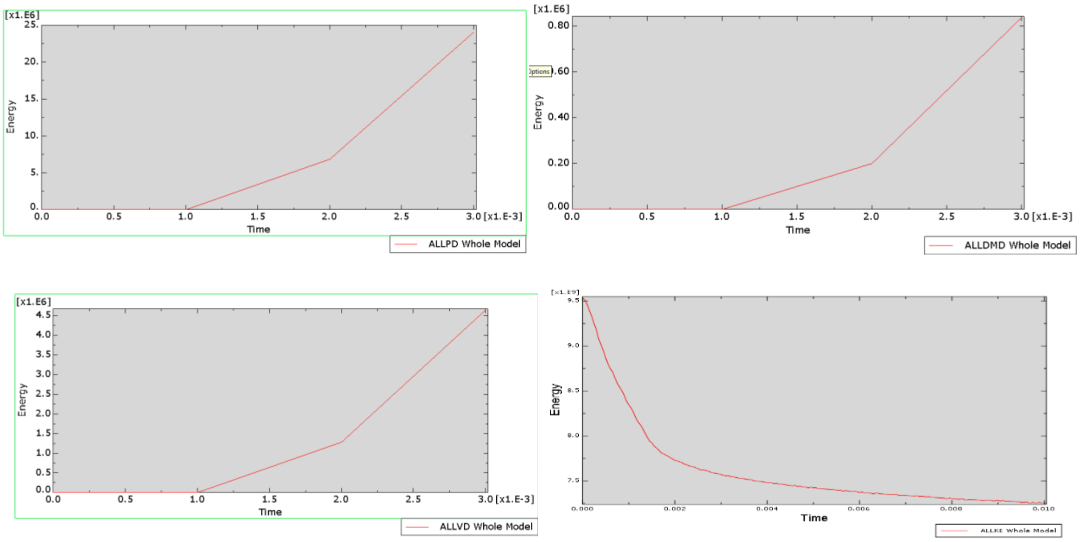

At 200m/s (Kinetic Energy lost=3.69e+09 J), (Total Energy dissipated=3.83e+9 J) & (Pitch Angle = 15˚).

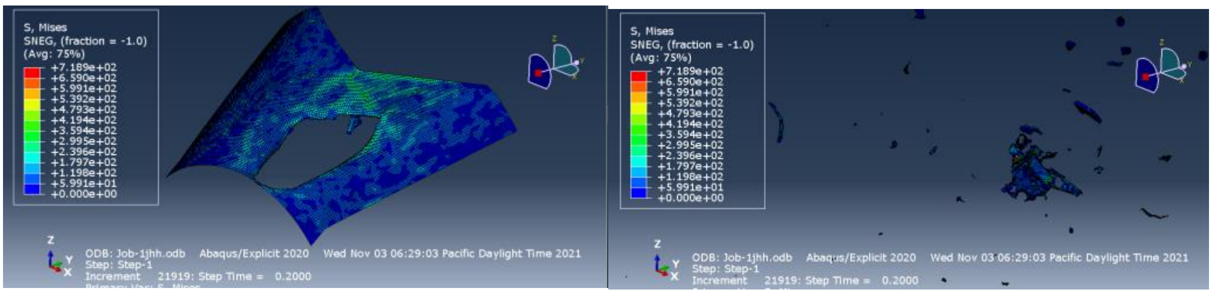

Pressure points (red points) isolated on the boundary conditions encastred when U1, U2 and U3 are all zero at a velocity of 200m/s (depicts the front side view portion of the aluminum plate and the UAV segments after impact).

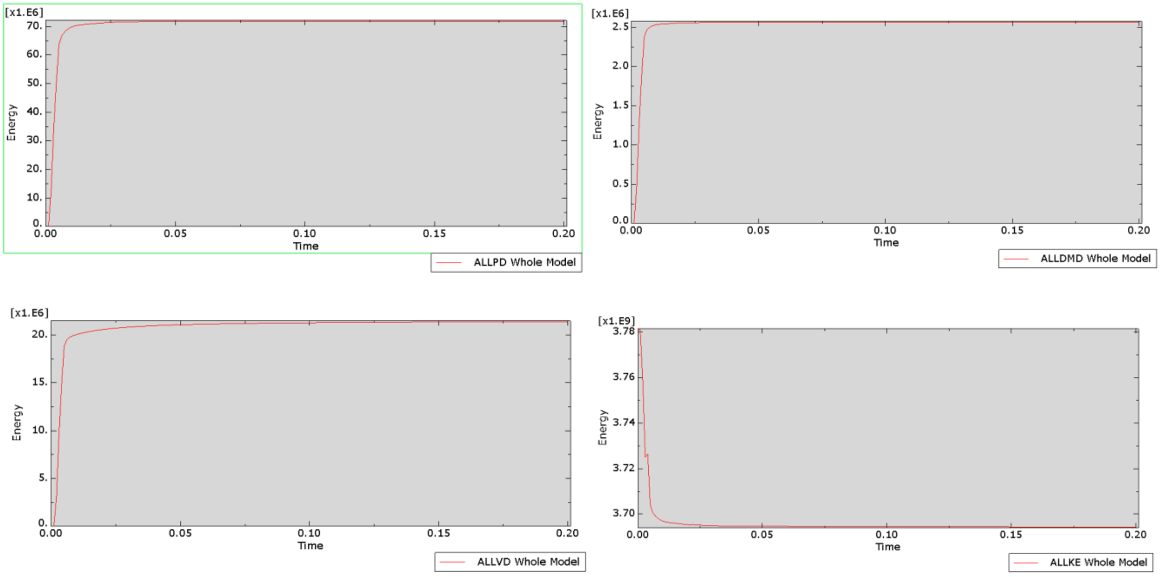

UAV impact on aircrafts can be a very dangerous and catastrophic event, and increasingly becoming common due to the increase in air traffic (Georgiadis 2008). According to document certification requirements, aviation structures have to be able to with stand drone impact scenarios, in order to enhance the overall structural integrity, performance and the passengers' safety. Because of the high relative velocity between the drone and airplane, drone collision event can be surely categorized as high velocity collision events, however the true classification of the impact events on regard to their velocity and energy is an extremely challenging case (Riccio 2016a; Caputo 2013; Riccio 2016b).

Element Quality Check for Meshing Purposes

Distorted isoparametric elements: angle between isoparametric lines is less than 45 ˚ or greater than 135˚. Tetrahedral quality measure: volume of tetrahedron divided by the volume of equilateral tetrahedron with same circum sphere radius; 0 for degenerate tetrahedron and 1 for equilateral tetrahedron. It is recommended that the tetrahedral quality measure be greater than 0.02, the min interior (dihedral) angle be greater than 10 ˚, and the max interior (dihedral) angle be less than 160 ˚. Modified tetrahedral quality measure: angles between the two-line segments on each edge; the edges of modified tetrahedral should be as straight as possible. It is recommended that the angle between the two-line segments on each edge is between 160 and 180 ˚. Triangular quality measure: area of triangle divided by the area of equilateral triangle with same circumcircle radius; 0 for degenerate triangle and 1 for equilateral triangle. It is recommended that the triangular quality measure be greater than 0.01, the min interior angle be greater than 10 ˚, and the max interior angle be less than 160 ˚. Nodal adjustments arising from contact interactions and/or tie constraints can cause severe element distortion. It may be necessary to remesh in order to reduce the amount of adjustment.

Energy Balance

Energy output is a vital part in Abaqus/Explicit analysis. Energy output comprises of several components, comparison between these various energy components is used to evaluate whether the analysis is having appropriate response.

The energy balance for the entire model can be written as;

$$E1 + Ev + EFD + EKE + E1HE - Ew - Epw - E1w - Emw - EHF = Etotal \quad (1)$$

where EI is the internal energy, EV is the viscous energy dissipated, EFD is the frictional dissipated energy, EKE is the kinetic energy, EIHE is the internal heat energy, EW is the work done by the external applied loads and EPW, ECW and EMW are the work done by contact penalties, constraint penalties and propelling added mass respectively. EHF is the external energy through external fluxes. The sum of these components is Etotal, which should be constant. However, for numerical models this is seldom the case, Etotal is only approximately constant [22], generally with an error of 1% [12].

The internal energy component, EI, in equation 1 is in turn composed of several other components. The expression for the internal energy is;

$$\boldsymbol{E1} = \boldsymbol{EE} + \boldsymbol{EP} + \boldsymbol{ECD} + \boldsymbol{EA} + \boldsymbol{EDMD} + \boldsymbol{EDC} + \boldsymbol{EFC}\ (\mathbf{2})$$

where EE is the recoverable elastic strain energy, EP is the dissipated energy through inelastic processes such as plasticity, ECD is the dissipated energy through viscoelasticity or creep, EA is the artificial strain energy, EDMD is the dissipated energy through damage, EDC is the dissipated energy through distortion control, EFC is the fluid cavity energy [12,22].

An important aspect to consider with extra care is the artificial strain energy. The artificial strain energy comprises of the energy stored in hourglass resistances and transverse shear in shell and beam elements. In order to decide whether a mesh refinement is required or not the artificial strain energy should be studied. Enormous values of artificial strain energy show that refinement or changes should be done.

6. RESULTS AND CONCLUSIONS

ALLKE, ALLDMD, ALLVD, and ALLPD [13]have shown the same energy incremental increase and decrease with time, whereas at 200 m/s where the flap pitching angle is 15˚ at take off which had the maximum takeoff throttle power at V1 (maximum takeoff velocity). At this phase after the impact collision the drone disintegrated into pieces with a kinetic energy loss of 3.69e+09 J which is considered the highest kinetic energy loss for the entire simulation the same applied for total internal energy lost which was around 3.83e+9 J. This goes together with the kinetic energy graph which shows a massive sarge in energy decrease which is exponential with time.

The damage dissipation energy graphs (ALLDMD) [13,14] for the whole model shows the level of severity that the UAV causes to the plate, studying the energy against time on these graphs helps to understand the magnitude of the impact that leaves the plate unsafe or unairworthy. At 116 m/s with a pitch angle of 33˚ the dissipation energy is at its minimum with a value of 100e+03 Joules approximately which is the lowest of all and at 171 m/s the levels are seen at 120e+03 Joules which shows a spike up of damage severity on the plate. However, at 15˚when the relative velocity is 116 m/s the damage dissipation value is at 1500e+03 Joules and when the relative velocity is 200 m/s the severity of the damage is seen to be very high at around 2500e+03 Joules concluding the analysis of the results that at flap angle of 15˚ which is considered the maximum pitch angle during takeoff where the engines are at a maximum throttle power the structural damage will be higher therefore resulting in an un airworthy structure.

The overall simulation results show that the go through phenomenon was found to exist in all of the cases in this paper, penetration of the plate structure is accompanied by segmented drone fragments flown unevenly, which has already threatened the airworthiness of aircraft. Thus, deemed necessary to investigate into different laws and regulations that place drone operations under a microscope and make significant and more policies that would guarantee the aircraft external and internal structure operation safe once the collision happens [18].

REFERENCES

1. Goraj, Z. Design Challenges Associated with Development of a New Generation UAV. Aircraft. Eng. Aerosp. Technol. 2005, 77, 361–368. [CrossRef]
2. D. Jenkins, B. Vasigh, The Economic Impact of Unmanned Aircraft Systems Integration in the United States, Association for Unmanned Vehicle Systems International (AUVSI), 2013, pp. 1–40.
3. Cambone, S.A.; Krieg, K.J.; Pace, P.; Wells, L., II. Unmanned Aircraft Systems Roadmap 2005–2030; U.S. Dept. of Defense: Washington, DC, USA, 2005.
4. Georgiadis S, Gunnion AJ, Thomson RS, Cartwright BK. UAV-strike simulation for certification of the Boeing 787 composite moveable trailing edge. Compos Struct 2008; 86:258–68.
5. FAA, General Operation and Flight Rules, FAR91.117, 2016.
6. FAA, Small UAS, FAR 107, 2016.
7. Cassada W, Liu J, Staley J. Aluminum alloys for aircraft structures. Adv Mater Processes 2002:27–9.
8. Warren AS. Developments and challanges for aluminium – A Boeing perspective. Mater Forum 2004; 28:24–31.
9. Børvik T, Hopperstad OS, Pedersen KO. Quasi-brittle fracture during structural impact of AA7075-T651 aluminium plates. Int J Impact Eng 2010;37(5):537-551.
10. Dorogoy A, Karp B, Rittel D. A Shear Compression Disk Specimen with Controlled Stress Triaxiality under Quasi-Static Loading. Exp Mech 2011;51(9):1545-1557.
11. Zaera R. Ballistic Impacts on Polymer Matrix Composites, Composite Armor, Personal Armor In: Abrate S, editor. Impact Engineering of Composite Structures, vol. 526: Springer Vienna; 2011. p. 305-403.
12. Dassault Syst`emes. Abaqus 6.14 Online Documentation: 9.6.1 Statement of energy balance. Dassault Syst`emes, http://abaqus.sys.kth.se/v6.14/books/gsa/ default.htm, 2014.
13. Dassault Syst`emes. Abaqus 6.14 Online Documentation: 1.1 The Abaqus products. Dassault Syst`emes, http://server-ifb147.ethz.ch:2080/v6.14/books/ gsa/default.htm, 2014.
14. Dassault Syst`emes. Abaqus 6.14 Online Documentation: 9.2.1 Explicit time integration. Dassault Syst`emes, http://abaqus.sys.kth.se/v6.14/books/gsa/ default.htm, 2014.
15. Dassault Syst`emes. Abaqus 6.14 Online Documentation: 2.4.1 Choosing between implicit and explicitanalysis.DassaultSyst`emes,http://serverifb147.ethz.ch:2080/v6.14/books/gsa/default.htm, 2014.
16. Dassault Syst`emes. Abaqus 6.14 Online Documentation: 9.2.3 Advantages of the explicit time integrationmethod.DassaultSyst`emes,http://abaqus.sys.kth.se/v6.14/books/gsa/default.htm, 2014.
17. Dassault Syst`emes. Abaqus 6.14 Online Documentation: 9.3.4 Mass scaling to control time incrementation. Dassault Syst`emes, http://abaqus.sys.kth.se/v6. 14/books/gsa/default.htm, 2014.

18. Xiaohua Lu, Xinchao Liu, Yulong Li, Yingchun Zhang, Hongfu Zuo. "Simulations of airborne collisions between drones and an aircraft windshield", Aerospace Science and Technology, 2020.

a. Smojver, D. Ivančević. "Numerical simulation of bird strike damage prediction in airplane flap structure", Composite Structures, 2010.

19. U. Srinivas Rao, L. Vijayaraghavan. "Revisiting size effect due to work of new surface formation in mechanical micro-machining using FEM", Materials Today: Proceedings, 2018.

20. Tolga Dursun, Costas Soutis. "Recent developments in advanced aircraft aluminium alloys", Materials & Design (1980-2015), 2014.

21. I Smojver. "Bird impact at aircraft structure – Damage analysis using Coupled Euler Lagrangian Approach", IOP Conference Series Materials Science and Engineering, 06/01/2010.

22. Quirino Estrada, Dariusz Szwedowicz, Jesús Silva-Aceves, Tadeusz Majewski, Julio Vergara-Vazquez, Alejandro Rodriguez-Mendez. "Crashworthiness behavior of aluminum profiles with holes considering damage criteria and damage evolution", International Journal of Mechanical Sciences, 2017.